





Right ventricular function as assessed by cardiac magnetic resonance imaging-derived strain parameters compared to high-fidelity micromanometer catheter measurements

Takahiro Sato¹, Bharath Ambale-Venkatesh², Stefan L. Zimmerman², Ryan J. Tedford³, Steven Hsu⁴, Ela Chamera⁴, Tomoki Fujii⁴ , Christopher J. Mullin⁵, Valentina Mercurio¹, Rubina Khair¹, Celia P. Corona-Villalobos², Catherine E. Simpson¹ , Rachel L. Damico¹, Todd M. Kolb¹, Stephen C. Mathai¹, Joao A.C. Lima⁴, David A. Kass⁴, Ichizo Tsujino⁶  and Paul M. Hassoun¹ 

¹Division of Pulmonary and Critical Care Medicine, Department of Medicine, Johns Hopkins University School of Medicine, Baltimore, MD, USA; ²Department of Radiology and Radiological Science, Johns Hopkins University School of Medicine, Baltimore, MD, USA; ³Division of Cardiology, Department of Medicine, Medical University of South Carolina, Charleston, SC, USA; ⁴Division of Cardiology, Department of Medicine, Johns Hopkins University School of Medicine, Baltimore, MD, USA; ⁵Brown University Warren Alpert Medical School, Providence, RI, USA; ⁶First Department of Medicine, Hokkaido University Hospital, Sapporo, Japan

Abstract

Right ventricular function has prognostic significance in patients with pulmonary hypertension. We evaluated whether cardiac magnetic resonance-derived strain and strain rate parameters could reliably reflect right ventricular systolic and diastolic function in precapillary pulmonary hypertension. End-systolic elastance and the time constant of right ventricular relaxation tau, both derived from invasive high-fidelity micromanometer catheter measurements, were used as gold standards for assessing systolic and diastolic right ventricular function, respectively. Nineteen consecutive precapillary pulmonary hypertension patients underwent cardiac magnetic resonance and right heart catheterization prospectively. Cardiac magnetic resonance data were compared with those of 19 control subjects. In pulmonary hypertension patients, associations between strain- and strain rate-related parameters and invasive hemodynamic parameters were evaluated. Longitudinal peak systolic strain, strain rate, and early diastolic strain rate were lower in PAH patients than in controls; peak atrial-diastolic strain rate was higher in pulmonary hypertension patients. Similarly, circumferential peak systolic strain rate was lower and peak atrial-diastolic strain rate was higher in pulmonary hypertension. In pulmonary hypertension, no correlations existed between cardiac magnetic resonance-derived and hemodynamically derived measures of systolic right ventricular function. Regarding diastolic parameters, tau was significantly correlated with peak longitudinal atrial-diastolic strain rate ($r = -0.61$), deceleration time ($r = 0.75$), longitudinal systolic to diastolic time ratio ($r = 0.59$), early diastolic strain rate ($r = -0.5$), circumferential peak atrial-diastolic strain rate ($r = -0.52$), and deceleration time ($r = 0.62$). Strain analysis of the right ventricular diastolic phase is a reliable non-invasive method for detecting right ventricular diastolic dysfunction in PAH.

Keywords

pulmonary arterial hypertension, strain and strain rate, right ventricular failure, pressure volume loop, tau

Date received: 7 April 2021; accepted: 17 June 2021

Pulmonary Circulation 2021; 11(3) 1–10

DOI: 10.1177/20458940211032529

Introduction

In pulmonary arterial hypertension (PAH), a chronic elevation of pulmonary arterial pressure causes progressive right ventricular (RV) dysfunction leading to significant morbidity and premature death.^{1,2} Accurate evaluation of RV morphology and function is critical in the management of PAH

Corresponding author:

Paul M. Hassoun, Division of Pulmonary and Critical Care Medicine, 1830 E. Monument Street, Baltimore, MD 21205, USA.

Email: phassoun@jhmi.edu



Creative Commons Non Commercial CC BY-NC: This article is distributed under the terms of the Creative Commons Attribution-NonCommercial 4.0 License (<https://creativecommons.org/licenses/by-nc/4.0/>) which permits non-commercial use, reproduction and distribution of the work without further permission provided the original work is attributed as specified on the SAGE and Open Access pages (<https://us.sagepub.com/en-us/nam/open-access-at-sage>).

© The Author(s) 2021
Article reuse guidelines:
sagepub.com/journals-permissions
journals.sagepub.com/home/pul



considering that RV failure is the leading cause of death in this syndrome. While there is no consensus on the best method for assessing RV function in patients with PAH, recent studies have demonstrated the prognostic value of some non-invasive measures, including echocardiography-derived tricuspid annular plane systolic excursion³ and cardiac magnetic resonance (CMR)-based assessment of RV ejection fraction.⁴

RV strain and strain rate (SR), which can be obtained from CMR and calculated from feature tracking (or multimodality tissue tracking), have emerged as powerful tools to accurately quantify myocardial mechanics in various regional segments and directions.⁵ Furthermore, RV strain analysis has been shown to be a useful tool for assessing disease severity and prognosis in patients with PAH.^{6–9}

Invasive indices based on micromanometer catheter measurements remain the gold standard references in the evaluation of global RV systolic¹⁰ and diastolic function.¹¹ However, these indices have only been used in a limited number of studies for RV assessment in PAH^{12,13} because of their invasiveness and need for special setups and expertise.

In this context, we aimed to ascertain whether CMR-based strain and SR imaging could provide accurate assessment of RV systolic and diastolic function in PAH patients. Accordingly, we first measured CMR-derived strain and SR parameters of PAH patients and compared them with those of age- and sex-matched subjects, using data from the multiethnic study of atherosclerosis subjects (MESA).¹⁴ We then aimed to directly compare the strain and SR parameters from CMR (performed within 5 h of catheterization) with invasive indices obtained by high-fidelity micromanometer catheter measurements in PAH patients.

Methods

We enrolled patients with known or suspected PH referred for right heart catheterization (RHC) and same-day CMR from January 2013 to March 2016 at our Hospital. Patients with precapillary PH at RHC were eligible for inclusion in this analysis. Precapillary PH was defined as a mean pulmonary artery pressure ≥ 25 mmHg and pulmonary vascular resistance >3 Wood Units, with pulmonary artery wedge pressure ≤ 15 mmHg during right heart catheterization.¹⁵ The research protocol was conducted in accordance with the Declaration of Helsinki and was approved by our Institutions Institutional Review Board. Informed consent was obtained from all patients. Age- and sex-matched subjects without cardiac and/or respiratory diseases from the MESA 4 study were included as controls for comparison. Baseline clinical characteristics were obtained from standardized clinic data prospectively obtained from our University Pulmonary Hypertension Registry.

CMR imaging

Volumetric cine images were acquired and analyzed to assess left ventricular (LV) and RV mass and function. All CMR images were read at our University by two investigators (C.P.C.-V. and S.L.Z.) blinded to the subjects and study timing. The cine imaging was steady-state free-precession cine imaging. A short-axis stack of 8–10 slices covering the entire ventricle, and 2 long-axis cine loops of 2- and 4-chamber views were obtained. Typical imaging parameters were slice thickness 6–8 mm, field of view 32–36 cm, minimum TR/TE, pixel size 1.4 x 1.4 mm, and temporal resolution <50 ms. CMR was performed within 5 h of catheterization.

Tissue-tracking CMR

We used offline semi-automated multimodality tissue-tracking software version 6.0 (Toshiba, Tokyo, Japan) to analyze the RV strain and SR. Multimodality tissue tracking reads characteristic pixel patterns in each 10×10 mm area as template blocks from the reference image. A search is performed in the next frame to find image blocks that best match the template block, such that the best match minimizes the mean squared error of the image pixel intensity (between current image block and template block). This procedure was repeated for all pixels in each image and for each frame to track moving pixels through the whole cardiac cycle.^{5,16,17} After uploading the CMR image, its brightness was optimized to ensure optimal endocardial/blood pool discrimination. The endocardial and epicardial borders of the ventricle were then manually traced on the end-diastolic frame, and the software automatically propagated the borders through the cardiac cycle. Adjustment of the tracked border was performed, as necessary, after visual assessment during cine loop playback by the reader.

RV longitudinal strain and SR data were directly obtained from cine images in the 4-chamber view (Fig. 1a). RV circumferential strain and SR data were obtained at mid-cavity level from short-axis images (Fig. 1b). A negative strain value indicates shortening with respect to the reference configuration at end-diastole, defined as the peak of the R wave on surface electrocardiography. Fig. 1c and d shows representative strain images of the control and PAH group, respectively. RV peak systolic strain was identified from the strain curve. Systolic time and diastolic time were also obtained from the strain analysis (Fig. 1c and d). Systolic to diastolic duration ratio (S:D ratio) was calculated as systolic time divided by diastolic time intervals from the strain curve. Fig. 1e and f shows representative SR images of the control and PAH subjects, respectively. Peak systolic strain rate (SRs), peak early diastolic strain rate (SR_e), peak atrial-diastolic strain rate (SR_a), and deceleration time (DT) of SR_e were obtained from the SR curve.

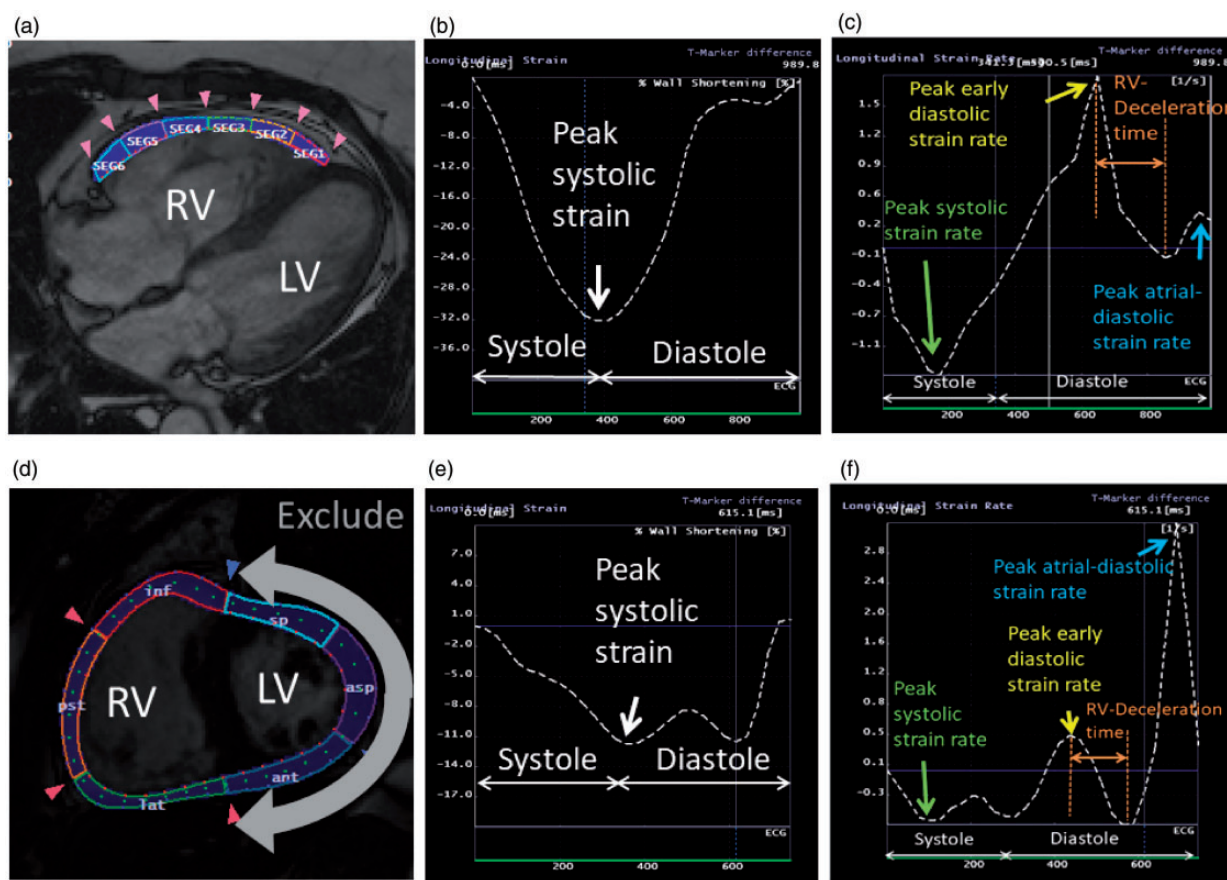


Fig. 1. (a) Representative image of right ventricular (RV) longitudinal peak systolic strain and peak strain rate in the 4-chamber view. (b) Representative image of RV circumferential peak strain and strain rate measurement in the short axis view at the mid-level. RV and left ventricular free wall were traced as a whole after the confirmation of six segments. Thereafter, three left ventricular free wall segments were excluded. (c) Representative strain curve image of control subjects. (d) Representative strain curve image of patients with pulmonary arterial hypertension. Peak systolic strain, systolic time, and diastolic time were identified from the strain curve. (e) Representative strain rate curve image of control subjects. (f) Representative strain rate image of image of patients with pulmonary arterial hypertension. Peak systolic strain rate, peak early diastolic strain rate (SRe), peak atrial-diastolic strain rate, and deceleration time of SRe were also analyzed from the strain rate curve.

Pressure volume analysis

The RV volume signal was calibrated to resting RV volume measurements obtained by same-day CMR. End-systolic pressure volume points were determined from a set of loops with varying preload volumes during phase 2 of the Valsalva maneuver, and fit by perpendicular regression using an iterative algorithm to derive the slope (end-systolic elastance, E_{es} , which is a gold standard for evaluating systolic function) of the end-systolic pressure volume relationship. This slope was then applied to the resting pressure volume loop to determine the x intercept (V_0) of the end-systolic pressure volume relationship, as described.¹² Effective arterial elastance (E_a), which is a gold standard for assessing afterload, was determined by dividing end-systolic pressure by stroke volume. RV-pulmonary artery coupling was assessed by the E_{es}/E_a ratio. Tau, which is the time constant of RV relaxation, was also calculated. Representative images of micromanometer catheter

measurements of E_{es} , E_a , and tau are shown in Supplemental Figure 1.

Data analysis

CMR measurements were compared between control subjects and PH patients. To identify CMR parameters most reflective of systolic function, correlation analyses were performed between hemodynamically derived E_{es} and global RV measures (RV ejection fraction, RV end-diastolic volume, and RV mass), as well as measures of RV systolic function (peak longitudinal systolic strain, peak longitudinal SRs, peak circumferential systolic strain, peak circumferential SRs, and S:D ratio). We also correlated E_a and E_{es}/E_a with these CMR parameters. To identify CMR parameters most reflective of diastolic function, correlation analyses were performed between hemodynamically derived tau, global RV measures, and measures of RV diastolic function (peak longitudinal SRe, peak longitudinal SRa, longitudinal

DT of SRe, longitudinal S:D ratio, peak circumferential SRe, peak circumferential SRa, circumferential DT of SRe, and circumferential S:D ratio).

Statistical methods

Categorical variables are expressed as percentages, and continuous variables are expressed as mean \pm SD for normally distributed variables or as medians with interquartile ranges for non-normal distributions. Departures from normality were detected with the Shapiro–Wilk statistic. In case of a difference in distribution between the control and PH groups, we added the interquartile range data to adequately compare these two groups. Differences in measurements between the control and PH groups were assessed with Fisher’s exact test, Student’s *t* test, or the Wilcoxon test as appropriate. Pearson correlation coefficients were used to determine correlations between continuous variables. Log transformations were performed as necessary to normalize distributions before correlation analysis. A two-sided *P*-value of <0.05 was considered significant throughout the analyses.

Given estimations based on previous studies¹⁸ that the correlation coefficient between CMR-derived strain parameters and pressure volume loop-derived systolic and diastolic parameters was 0.6 or greater, using a two-sided test, 5% significance level ($\alpha=0.05$) with 80% power ($\beta=0.2$), the required sample size was estimated to be approximately 19 individuals.¹⁹

The intra-observer agreement for measurements was assessed by comparing the measurements of repeated analysis in 10 randomly chosen subjects (T.S.). The inter-observer agreement was assessed using the same patients by comparing the results measured by T.S. and those obtained by an experienced reader (T.F.). The second reader was not aware of the CMR measurements of the first examiner. Bland–Altman analysis and intraclass correlations between the two measurements were used to assess reproducibility.

All statistical analyses were performed using JMP® Version 11 (SAS Institute Inc., Cary, NC).

Results

Study population and demographics

Sixteen PAH patients and three patients with precapillary PH due to systemic sclerosis-related interstitial lung disease (SSc-ILD) met the entry criteria during the study period. Of the 16 PAH patients, six were diagnosed with idiopathic PAH, and 10 were diagnosed with SSc-associated PAH. Patients with SSc-associated PH met the American College of Rheumatology/European League Against Rheumatism diagnostic criteria for systemic sclerosis.²⁰ The diagnosis of PH due to SSc-ILD was based on previously reported criteria.²¹ Nineteen age- and sex-matched healthy controls were included from the MESA 4 study.

There were no significant demographic differences between the PH and control groups (Table 1).

Among patients with PH, 18 (95%) were categorized as World Health Organization functional class II or III (Table 2). The mean pulmonary artery pressure was 33 mmHg, and pulmonary vascular resistance was 5.5 Wood Units (Table 2).

Comparison of CMR parameters between the control and PH groups

Table 1 shows the comparison of CMR parameters between the control and PH groups. PH patients exhibited significantly greater RV end-diastolic volume, RV end-systolic volume, and RV mass compared to controls. RV ejection fraction and LV mass were lower in PH patients than in control subjects.

For strain-related parameters, RV peak longitudinal systolic strain, RV peak longitudinal SRs, RV peak longitudinal SRe, and RV peak circumferential SRs were significantly decreased in PH patients than in controls. In contrast, RV peak longitudinal SRa and peak circumferential SRa were higher in PH patients than in controls. Both longitudinal and circumferential S:D ratios were higher in PH patients than in controls.

Correlations between invasive parameters and CMR indices of the right ventricle

There was no significant correlation between invasively measured E_{es} or E_{es}/E_a , and longitudinal CMR measures of systolic function; likewise, there was no correlation between E_{es} or E_{es}/E_a and circumferential CMR systolic measures. Log E_a was significantly correlated with RV longitudinal systolic strain ($r=0.46$, $P=0.0498$) alone (Supplemental Figure 2). Fig. 2 shows relationships between tau and CMR-derived strain, SR, and S:D ratio. For RV longitudinal analysis, tau was significantly correlated with RV peak longitudinal SRa ($r=-0.61$, $P=0.006$), RV peak longitudinal SRe of DT ($r=0.75$, $P=0.0002$), and longitudinal S:D ratio ($r=0.59$, $P=0.0083$). In circumferential analysis, tau was significantly correlated with RV peak circumferential SRe ($r=-0.5$, $P=0.027$), RV peak circumferential SRa ($r=-0.52$, $P=0.0257$), and RV peak circumferential SRe of DT ($r=0.62$, $P=0.0058$).

Reproducibility

Limits of agreement analyzed from Bland–Altman analysis of intra-observer variability of strain and SR indices and intraclass correlations are shown in Supplemental Table 1. Intraclass correlations were greater than 0.9, and the limit of agreement was within 5% in all of the 20 indices. Limits of agreement and intraclass correlation coefficients for inter-observer variability are shown in Supplemental Table 2. Intraclass correlations were similarly high, with

Table 1. Demographics of participants.

Parameters	Controls (n = 19)	Patients with PH (n = 19)	P-value
Age (years)	57 ± 5	56 ± 13	0.644
Sex (male/female)	3/16	3/16	1.00
Body surface area (m ²)	1.81 ± 0.18	1.82 ± 0.21	0.82
Race (white/non-white)	11/8	16/3	0.0625
Systolic systemic blood pressure (mmHg)	119 ± 19	125 ± 19	0.3261
Diastolic systemic blood pressure (mmHg)	71 ± 10	71 ± 10	0.8263
Hypertension (n)	1	3	0.6039
Hyperlipidemia (n)	1	3	0.6039
Diabetes mellitus (n)	2	1	1.000
Right ventricular measurements			
End-diastolic volume (ml)	105 ± 20	171 ± 57	<0.0001
End-systolic volume (ml)	45 ± 11	95 ± 39	<0.0001
Mass (g)	20 ± 4	27 ± 8	0.003
Ejection fraction (%)	57 ± 5	45 ± 9	<0.0001
Left ventricular measurements			
End-diastolic volume (ml)	130 ± 25	114 ± 25	0.0641
End-systolic volume (ml)	52 ± 16	46 ± 11	0.1616
Mass index (g)	116 ± 23	82 ± 18	<0.0001
Ejection fraction (%)	60 ± 8	60 ± 6	0.9257
Right ventricular strain measurements			
Longitudinal peak systolic strain (%)	-31 ± 4.6	-24.5 ± 6.4	0.0001
Longitudinal peak systolic strain rate (m/s)	-1.42 ± 0.22	-1.09 ± 0.29	0.0003
Longitudinal early diastolic strain rate (m/s)	2.12 ± 0.66	0.74 ± 0.37	<0.0001
Longitudinal peak atrial-diastolic strain rate (m/s)	0.69 ± 0.44	1.5 ± 1.13	0.0382
Longitudinal deceleration time of early diastolic strain rate (ms)	193 (138–233)	119 ± 29	<0.001
Longitudinal R-R interval (ms)	921 ± 124	846 ± 145	0.954
Longitudinal systolic time (ms)	345 ± 34	371 ± 63	0.1196
Longitudinal diastolic time (ms)	576 ± 114	475 ± 86	0.0038
Longitudinal systolic to diastolic duration ratio	0.62 ± 0.14	0.78 ± 0.1	<0.0001
Circumferential peak systolic strain (%)	-14 ± 2.8	-12.2 ± 3.1	0.728
Circumferential peak systolic strain rate (m/s)	-0.66 ± 0.17	-0.48 ± 0.15	0.0045
Circumferential early diastolic strain rate (m/s)	0.77 ± 3	0.72 ± 0.34	0.587
Circumferential peak atrial-diastolic strain rate (m/s)	0.25 ± 0.08	0.31 (0.26–0.52)	0.0078
Circumferential deceleration time of early diastolic strain rate (ms)	226 ± 59	169 ± 74	0.0135
Circumferential R-R interval (ms)	912 ± 117	833 ± 137	0.0655
Circumferential systolic time (ms)	350 ± 39	408 ± 65	0.0021
Circumferential diastolic time (ms)	562 ± 101	426 ± 98	0.0002
Circumferential systolic to diastolic duration ratio	0.64 ± 0.11	1.0 ± 0.2	<0.0001

PH: pulmonary hypertension.

coefficients >0.9 in all indices except three (RV longitudinal SRe, 0.87, RV circumferential SRe, 0.87, and RV circumferential DT, 0.89). Limits of agreement were within 5% in all 20 indices.

Discussion

In the present study, we compared CMR measures of RV function, including strain parameters, between 19 PH patients and 19 controls, and we examined relationships between CMR-measured RV systolic and diastolic function and invasively measured gold standard parameters of RV systolic and diastolic function in PH patients. The main findings of this study were (1) CMR-derived strain-related

parameters were substantially different between PH and control groups, both longitudinally and circumferentially; (2) there was no significant correlation between CMR parameters of RV systolic function and invasively measured E_{es} in PH patients; (3) CMR parameters of RV diastolic function were correlated with tau, with peak atrial-diastolic SR and DT being the strongest correlates; and (4) S:D ratio derived from CMR strain was correlated with tau, but not with E_{es} .

In PH patients, RV function is a major determinant of survival. Both systolic and diastolic functions play important roles in RV performance, and both should be considered as important individual determinants of overall function. However, most studies to date have focused on

Table 2. Characteristics of patients with pulmonary arterial hypertension.

Diagnosis	
IPAH	6 (32%)
SSc-PAH	10 (53%)
SSc-ILD-PH	3 (16%)
WHO-functional class	
I	1 (5%)
II	7 (37%)
III	11 (58%)
Pulmonary hemodynamics	
Systolic pulmonary artery pressure (mmHg)	53 (44–82)
Diastolic pulmonary artery pressure (mmHg)	21 (16–30)
Mean pulmonary artery pressure (mmHg)	33 (27–49)
Pulmonary capillary wedge pressure (mmHg)	8 ± 3
Right ventricular end-diastolic pressure (mmHg)	7 (5–10)
Mean right atrial pressure (mmHg)	5 (4–8)
Cardiac index (L/min/m ²)	2.4 ± 0.5
Pulmonary vascular resistance (Wood Units)	5.5 (4.5–9)
Use of pulmonary hypertension-specific vasodilators	
Prostanoid	0 (0%)
PDE-5 inhibitor	8 (42%)
Endothelin receptor antagonist	4 (21%)
Calcium channel blocker	7 (37%)
Diuretics	10 (53%)
None	5 (26%)
Brain natriuretic peptide (pg/ml)	205 (130–526)
Micromanometer catheter measurements	
RV afterload	
Effective arterial elastance (E _a)	0.71 (0.65–1.11)
RV systolic function	
End-systolic elastance (E _{es})	0.62 (0.43–0.96)
RV-pulmonary arterial coupling	
E _{es} /E _a	0.78 (0.45–1.04)
RV diastolic function	
Tau (ms)	32.5 ± 11.3

IPAH: idiopathic PAH; SSc-PAH: scleroderma-associated PAH; SSc-ILD-PH: scleroderma with interstitial lung disease and PH; WHO: World Health Organization; PDE: phosphodiesterase; RV: right ventricular.

RV systolic function,^{4,8,22,23} with few studies concentrating on RV diastolic dysfunction in PH. Imaging measures of RV systolic performance, however, have many clinical pitfalls. RV ejection fraction, for example, is known to be an insensitive measure of RV contractile performance, and correlates poorly with intrinsic, load-independent measurements of RV contractile function.^{12,24} This is because preload and afterload significantly impact RV contractility as assessed by non-invasive imaging. Similar to these findings, the present study shows no association between CMR measures of systolic function and invasively derived measures of load-independent contractile function.

Although CMR measures of systolic function fall short, CMR-derived RV diastolic measurements may in fact prove more clinically useful. In the present study, we demonstrated that diastolic RV SR, as measured by CMR, was quite different between controls and PH patients. Moreover,

multiple diastolic indices were significantly correlated with invasively measured tau. These findings indicate that CMR-derived strain analysis could allow for non-invasive evaluation of RV diastolic function, particularly relaxation represented by tau, in PH.

Among RV diastolic strain or SR examined in this study, peak longitudinal SR_a and peak circumferential SR_a were higher in PH patients than in controls and were most strongly correlated with tau. There are several possible reasons why both longitudinal and circumferential RV SR_a were elevated in our PH patients. For example, RV SR_a reflects RV stiffness and right atrial contraction. Thus, RV SR_a can theoretically increase either by RV stiffening or by augmented right atrial contraction. Indeed, recent CMR studies on PAH patients have reported a stiffened right ventricle²⁵ and increased right atrial contractility.²⁶ Thus, sustained afterload to the right heart might have caused RV hypertrophy and stiffening and a compensatory

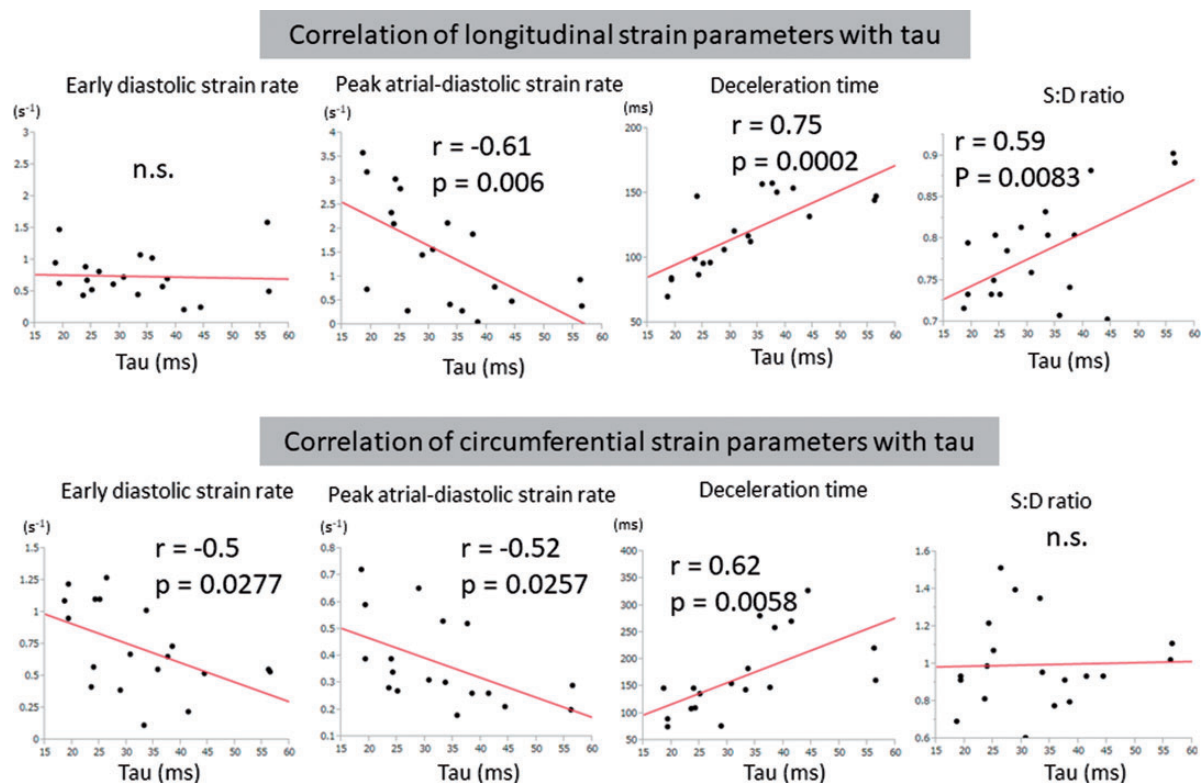


Fig. 2. Correlations between tau and cardiac magnetic resonance-derived strain and strain rate parameters. S:D: systolic to diastolic duration

increase in right atrial contraction, with a subsequent increase in SRa in our PH cohort.

The correlation analysis indicated a negative association between RV SRa and tau in both longitudinal and circumferential analysis. Our results are consistent with a previous study by Okumura et al.,¹⁸ where tau and SRa showed an inverse relationship. Notably, a recent study reported that right atrial contraction was increased in patients with mild PH compared to controls, yet decreased in patients with advanced PH.²⁶ This “non-linear” relationship between right atrial contraction and the progression of PH might have caused an inverse relationship between RV SRa and tau. Another explanation could be that the two indices reflect different phases of RV diastole; tau is an early diastolic index, whereas RV SRa is a late diastolic parameter. This may have caused the lack of a linear positive relationship between the two indices seen in our study.

Previous echocardiographic studies have shown a mild correlation between longitudinal early diastolic SR and tau in children with congenital heart disease-associated PAH.¹⁸ In contrast, in the present study, there was no significant association between the two indices. This may be due to differences in age or PH type of the participants, or to the different modalities used, i.e. echocardiography versus CMR, in the two studies. However, there was a significant correlation between circumferential peak SRe and tau in our CMR study, suggesting that circumferential

strain indices may reflect RV diastolic dysfunction in a different manner compared with longitudinal parameters. CMR has become an established modality and the gold standard for evaluating right heart in patients with PH, but in recent years, 3D echocardiography has made it possible to evaluate strain in the entire right ventricle and in various directions,^{27–29} which make assessment of right ventricular contractility and diastolic function possible.

Tello et al.³⁰ have recently documented significant associations of RV longitudinal or radial peak strain with E_{es}/E_a , E_a , and Tau in 38 precapillary PH patients. Similar to our study, these findings indicate potential reliability of CMR-derived strain analysis for the assessment of RV function in PH patients. However, only peak strain was analyzed in this study by Tello et al., whereas strain rate was not. Thus, further evaluation for more appropriate use of different types of strain and strain rate indices is needed.

S:D ratio is an indicator of global ventricular performance. Recently, high S:D ratio of the left ventricle was found associated with poor prognosis in patients with dilated cardiomyopathy, and a similar predictive value of RV S:D ratio has also been demonstrated in PAH.^{31,32} In our study, a high longitudinal S:D ratio was correlated with an increased tau, consistent with the recent echocardiographic report by Okumura et al.¹⁸ A similar positive correlation with tau was observed for DT in the present study. These findings suggest that time-related indices of CMR

strain analysis could be used to evaluate RV diastolic function and prognosis in PAH.

Studies on patients with left heart disease³³ and rodent experimental models^{34,35} have demonstrated significant correlations between pressure volume loop analysis-derived E_{es} and echocardiography-derived peak systolic strain or SR of the left ventricle. However, in our study, significant correlations between E_{es} and CMR-derived parameters of RV systolic function, such as peak systolic strain and SR, were not found. Tello et al.³⁰ also failed to find a correlation between E_{es} and peak RV strain rate. The inconsistency between previous studies and ours may be due to the difference in the ventricle examined, i.e. left versus right ventricle, or to vendor-³⁶ or modality-specific variability, i.e. echocardiography versus CMR. In addition, there is a possibility that indices of strain analysis may reflect subtle or certain specific changes in RV function that cannot be detected by E_{es} . Importantly, a recent report by Kraigher-Krainer et al.³⁷ revealed decreased left ventricular longitudinal and circumferential strain indices in patients with heart failure whose LV ejection fraction was preserved. In addition, recent studies have reported significant associations between RV peak systolic strain and disease severity^{6,38} or mortality^{7,8} in PH. Thus, the clinical relevance of systolic strain and SR needs to be further evaluated in diverse PH types and in larger prospective studies.

In the present study, RV longitudinal peak systolic strain was significantly correlated with E_a . This is consistent with a recent echocardiographic study demonstrating a close correlation between RV free wall strain and pulmonary arterial pressure in PAH.³⁹ Taken together, these studies suggest that RV strain during systole is increased in response to an elevated RV afterload, and could be a unique marker of RV response to an increased afterload in PH. Alternatively, strain-related indices were not correlated with E_{es}/E_a in our study. E_{es}/E_a is a powerful load-independent indicator of RV-pulmonary artery coupling.^{12,24} Thus, our data indicated a limited sensitivity of RV strain-related CMR parameters for the assessment of RV-pulmonary artery coupling in PH.

While this was a prospective study for which a power analysis was performed to calculate the sample size needed to establish correlations between CMR parameters and invasive parameters, it included a small number of patients from a single center. In addition, for obvious reasons, pressure volume loops were not obtained in control subjects. Furthermore, CMR and right heart catheterization were not performed contemporaneously, which potentially hampered an accurate comparison of the techniques. However, all patients were in stable clinical condition, and the two studies were performed within 5 h. This study included a combination of patients with idiopathic PAH, SSc-associated PAH, and precapillary PH due to SSc-ILD, which might have also affected the results. Finally, variations in treatment regimens might have also influenced

the results, as PAH-specific vasodilators may affect cardiac function.⁴⁰

In conclusion, the present study demonstrated differences in various CMR parameters including strain and SR between control subjects and PH patients. Notably, there was no significant correlation between E_{es} , the gold standard for the assessment of systolic function, and CMR strain parameters of RV systolic function. In contrast, there were significant correlations between tau and CMR-derived strain measures of the right ventricle, such as longitudinal SRe, longitudinal and circumferential SRA, DT of SRe, and longitudinal S:D ratio. These suggest that strain analysis using CMR is most appropriate to assess diastolic function in PAH.

Conflict of interest

The author(s) declared the following potential conflicts of interest with respect to the research, authorship, and/or publication of this article: PMH has served on a Scientific Advisory Board for Merck & Co..

Authors' contributions

TS, BA-V, RJT, SH, VM, CJM, VM, JA CL, PMH, DAK, and IC intellectually contributed to the analysis and interpretation of data; SLJ, EC, and TF managed the overall CMR imaging and assessment; RK, CES, RLD, TMK, and SCM contributed to the design data and acquisition; PMH gave final approval of the manuscript submitted.

Ethical approval

The research protocol was approved by the Johns Hopkins Medical Institutions Institutional Review Board, and informed consent was obtained from all patients.





Guarantor

Paul M. Hassoun.

Funding

The author(s) disclosed receipt of the following financial support for the research, authorship and/or publication of this article: The study was supported by The National Institutes of Health/ National Heart, Lung, and Blood Institute awards P50 HL084946 (PMH), HL114910 (PMH), and U01HL125175-01 (PMH), and by a fellowship grant from the Uehara Memorial Foundation, the Mochida Memorial Foundation for Medical and Pharmaceutical Research, the Ito Foundation for the Promotion of Medical Science, and the Japanese Society for the Promotion of Science (TS).

ORCID iDs

Tomoki Fujii  <https://orcid.org/0000-0002-4120-4435>
 Catherine E. Simpson  <https://orcid.org/0000-0002-2388-5660>
 Ichizo Tsujino  <https://orcid.org/0000-0002-0196-9572>
 Paul M. Hassoun  <https://orcid.org/0000-0003-0601-4975>

Supplemental material

Supplemental material for this article is available online.

References

- D'Alonzo GE, Barst RJ, Ayres SM, et al. Survival in patients with primary pulmonary hypertension. Results from a national prospective registry. *Ann Intern Med* 1991; 115: 343–349.
- Tonelli AR, Arelli V, Minai OA, et al. Causes and circumstances of death in pulmonary arterial hypertension. *Am J Respir Crit Care Med* 2013; 188: 365–369.
- Forfia PR, Fisher MR, Mathai SC, et al. Tricuspid annular displacement predicts survival in pulmonary hypertension. *Am J Respir Crit Care Med* 2006; 174: 1034–1041.
- van de Veerdonk MC, Kind T, Marcus JT, et al. Progressive right ventricular dysfunction in patients with pulmonary arterial hypertension responding to therapy. *J Am Coll Cardiol* 2011; 58: 2511–2519.
- Ohyama Y, Ambale-Venkatesh B, Chamera E, et al. Comparison of strain measurement from multimodality tissue tracking with strain-encoding MRI and harmonic phase MRI in pulmonary hypertension. *Int J Cardiol* 2015; 182: 342–348.
- Puwanant S, Park M, Popovic ZB, et al. Ventricular geometry, strain, and rotational mechanics in pulmonary hypertension. *Circulation* 2010; 121: 259–266.
- Sachdev A, Villarraga HR, Frantz RP, et al. Right ventricular strain for prediction of survival in patients with pulmonary arterial hypertension. *Chest* 2011; 139: 1299–1309.
- Fine NM, Chen L, Bastiansen PM, et al. Outcome prediction by quantitative right ventricular function assessment in 575 subjects evaluated for pulmonary hypertension. *Circ Cardiovasc Imaging* 2013; 6: 711–721.
- Hardegree EL, Sachdev A, Villarraga HR, et al. Role of serial quantitative assessment of right ventricular function by strain in pulmonary arterial hypertension. *Am J Cardiol* 2013; 111: 143–148.
- Kass DA, Maughan WL, Guo ZM, et al. Comparative influence of load versus inotropic states on indexes of ventricular contractility: experimental and theoretical analysis based on pressure-volume relationships. *Circulation* 1987; 76: 1422–1436.
- Matsubara H, Takaki M, Yasuhara S, et al. Logistic time constant of isovolumic relaxation pressure-time curve in the canine left ventricle. Better alternative to exponential time constant. *Circulation* 1995; 92: 2318–2326.
- Tedford RJ, Mudd JO, Girgis RE, et al. Right ventricular dysfunction in systemic sclerosis-associated pulmonary arterial hypertension. *Circ Heart Fail* 2013; 6: 953–963.
- Hsu S, Houston BA, Tampakakis E, et al. Right ventricular functional reserve in pulmonary arterial hypertension. *Circulation* 2016; 133: 2413–2422.
- Opdahl A, Ambale Venkatesh B, Fernandes VRS, et al. Resting heart rate as predictor for left ventricular dysfunction and heart failure: MESA (Multi-Ethnic Study of Atherosclerosis). *J Am Coll Cardiol* 2014; 63: 1182–1189.
- Galie N, Humbert M, Vachiery JL, et al. 2015 ESC/ERS Guidelines for the diagnosis and treatment of pulmonary hypertension: the Joint Task Force for the Diagnosis and Treatment of Pulmonary Hypertension of the European Society of Cardiology (ESC) and the European Respiratory Society (ERS); endorsed by: Association for European Paediatric and Congenital Cardiology (AEPC), International Society for Heart and Lung Transplantation (ISHLT). *Eur Respir J* 2015; 46: 903–975.
- Zareian M, Ciuffo L, Habibi M, et al. Left atrial structure and functional quantitation using cardiovascular magnetic resonance and multimodality tissue tracking: validation and reproducibility assessment. *J Cardiovasc Magn Reson* 2015; 17: 52.
- Imai M, Ambale Venkatesh B, Samiei S, et al. Multi-ethnic study of atherosclerosis: association between left atrial function using tissue tracking from cine MR imaging and myocardial fibrosis. *Radiology* 2014; 273: 703–713.
- Okumura K, Slorach C, Mroczek D, et al. Right ventricular diastolic performance in children with pulmonary arterial hypertension associated with congenital heart disease: correlation of echocardiographic parameters with invasive reference standards by high-fidelity micromanometer catheter. *Circ Cardiovasc Imaging* 2014; 7: 491–501.
- Machin D CM, Fayers PM, Pinol A. *Sample size tables for clinical studies*. 2nd ed. Malden, MA: Blackwell Science Ltd, 1997, pp.168–173.
- van den Hoogen F, Khanna D, Fransen J, et al. 2013 classification criteria for systemic sclerosis: an American College of Rheumatology/European League against Rheumatism collaborative initiative. *Arthr Rheumat* 2013; 65: 2737–2747.
- Le Pavec J, Girgis RE, Lechtzin N, et al. Systemic sclerosis-related pulmonary hypertension associated with interstitial lung disease: impact of pulmonary arterial hypertension therapies. *Arthr Rheumat* 2011; 63: 2456–2464.
- Vitarelli A, Mangieri E, Terzano C, et al. Three-dimensional echocardiography and 2D-3D speckle-tracking imaging in chronic pulmonary hypertension: diagnostic accuracy in detecting hemodynamic signs of right ventricular (RV) failure. *J Am Heart Assoc* 2015; 4: e001584.
- Mahran Y, Schueler R, Weber M, et al. Noninvasive model including right ventricular speckle tracking for the evaluation of pulmonary hypertension. *World J Cardiol* 2016; 8: 472–480.
- Vanderpool RR, Pinsky MR, Naeije R, et al. RV-pulmonary arterial coupling predicts outcome in patients referred for pulmonary hypertension. *Heart* 2015; 101: 37–43.
- Rain S, Handoko ML, Trip P, et al. Right ventricular diastolic impairment in patients with pulmonary arterial hypertension. *Circulation* 2013; 128: 2016–2025.
- Sato T, Tsujino I, Oyama-Manabe N, et al. Right atrial volume and phasic function in pulmonary hypertension. *Int J Cardiol* 2013; 168: 420–426.
- Murch SD, La Gerche A, Roberts TJ, et al. Abnormal right ventricular relaxation in pulmonary hypertension. *Pulmonary Circul* 2015; 5: 370–375.
- Atsumi A, Ishizu T, Kameda Y, et al. Application of 3-dimensional speckle tracking imaging to the assessment of right ventricular regional deformation. *Circ J* 2013; 77: 1760–1768.
- Ozawa K, Funabashi N, Takaoka H, et al. Utility of three-dimensional global longitudinal strain of the right ventricle using transthoracic echocardiography for right ventricular systolic function in pulmonary hypertension. *Int J Cardiol* 2014; 174: 426–430.
- Tello K, Dalmer A, Vanderpool R, et al. Cardiac magnetic resonance imaging-based right ventricular strain analysis for assessment of coupling and diastolic function in pulmonary hypertension. *JACC Cardiovasc Imaging* 2019; 12: 2155–2164.

31. Mondal T, Slorach C, Manlhiot C, et al. Prognostic implications of the systolic to diastolic duration ratio in children with idiopathic or familial dilated cardiomyopathy. *Circ Cardiovasc Imaging* 2014; 7: 773–780.
32. Alkon J, Humpl T, Manlhiot C, et al. Usefulness of the right ventricular systolic to diastolic duration ratio to predict functional capacity and survival in children with pulmonary arterial hypertension. *Am J Cardiol* 2010; 106: 430–436.
33. Yotti R, Bermejo J, Benito Y, et al. Validation of noninvasive indices of global systolic function in patients with normal and abnormal loading conditions: a simultaneous echocardiography pressure-volume catheterization study. *Circ Cardiovasc Imaging* 2014; 7: 164–172.
34. Kovacs A, Olah A, Lux A, et al. Strain and strain rate by speckle-tracking echocardiography correlate with pressure-volume loop-derived contractility indices in a rat model of athlete's heart. *Am J Physiol Heart Circ Physiol* 2015; 308: H743–748.
35. Ferferieva V, Van den Bergh A, Claus P, et al. Assessment of strain and strain rate by two-dimensional speckle tracking in mice: comparison with tissue Doppler echocardiography and conductance catheter measurements. *Eur Heart J Cardiovasc Imag* 2013; 14: 765–773.
36. Farsalinos KE, Daraban AM, Unlu S, et al. Head-to-head comparison of global longitudinal strain measurements among nine different vendors: the EACVI/ASE inter-vendor comparison study. *J Am Soc Echocardiogr* 2015; 28: 1171–1181.
37. Kraigher-Krainer E, Shah AM, Gupta DK, et al. Impaired systolic function by strain imaging in heart failure with preserved ejection fraction. *J Am Coll Cardiol* 2014; 63: 447–456.
38. Marwick TH. Measurement of strain and strain rate by echocardiography: ready for prime time? *J Am Coll Cardiol* 2006; 47: 1313–1327.
39. Wright L, Negishi K, Dwyer N, et al. Afterload dependence of right ventricular myocardial strain. *J Am Soc Echocardiogr* 2017; 30: 676–684.e671.
40. Guazzi M, Vicenzi M, Arena R, et al. PDE5 inhibition with sildenafil improves left ventricular diastolic function, cardiac geometry, and clinical status in patients with stable systolic heart failure: results of a 1-year, prospective, randomized, placebo-controlled study. *Circ Heart Fail* 2011; 4: 8–17.